JOURNAL OF MATERIALS SCIENCE 28 (1993) 3709–3714

Phonon scattering and thermal conduction mechanisms of sintered aluminium nitride ceramics

KOJI WATARI
Ceramics Science Department, Government Industrial Research Institute Nagoya, Hirate-cho, Kita-ku, Nagoya 462, Japan

KOZO ISHIZAKI
Department of Materials Science and Engineering, School of Mechanical Engineering, Nagaoka University of Technology, Nagaoka, Niigata 940-21, Japan

FUMIAKI TSUCHIYA
Mitsubishi Heavy Industries, Oye-cho, Minato-ku, Nagoya 455, Japan

From thermal diffusivity measurements of sintered AlN at temperatures ranging from 100 to 1000 K, the phonon mean free path of AlN was calculated in order to investigate phonon scattering mechanisms. The calculated mean phonon scattering distance was increased with decreasing temperature. The mean phonon–defect scattering distances were respectively limited to about 50 nm at temperatures ranging from 100 to 270 K and about 30 nm at temperatures ranging from 100 to 700 K, for AlN specimens with a room-temperature thermal conductivity of 220 and 121 $W m^{-1} K^{-1}$ containing 0.1 and 1.4 wt % oxygen, respectively. These short phonon–defect scattering distances were considered to correspond to the separation of oxygen-related internal defects in AlN grains. Calculation of the mean phonon scattering frequencies indicated that the phonon scattering is dominated by phonon–defect scattering at temperatures below 270 K for an AlN specimen with an oxygen content of 0.1 wt %, and at temperatures below 350 K for an AlN specimen with an oxygen content of 1.4 wt %.

1. Introduction

Aluminium nitride (AlN) ceramics are highly thermal-conductive non-metallic materials. The theoretical thermal conductivity of pure AlN is predicted to be 320 $W m^{-1} K^{-1}$ for a single crystal at room temperature [1, 2]. The thermal conductivity of polycrystalline AlN, however, is lowered by impurities such as oxygen [1–13], silicon, iron and magnesium [4], as well as silicon dioxide [14]. Among them, oxygen is the most deleterious and common impurity. The character of oxygen impurity in AlN single crystal and polycrystal was evaluated by using X-ray diffraction lattice measurements [1, 6, 12, 13], oxygen content measurements [1–11], thermal conductivity measurements [1–13], photoluminescence spectroscopy [12, 13] and transmission electron microscopy (TEM) [15–17].

For an AlN single crystal, the thermal conduction mechanism was found to be controlled by crystalline defects such as oxygen solute atoms and associated Al vacancies. Slack [1, 2] measured the thermal conductivity of AlN single crystals with various oxygen contents, and concluded that the phonon scattering was caused by mass defects of aluminium vacancies as $Al_{0.67}O$ in AlN.

In the case of sintered polycrystalline AlN, many authors believe that the reduction of thermal conductivity is due to oxygen-related defects in the AlN lattice and/or the oxide grain boundaries [3–6]. Because the thermal conductivity of the grain-boundary oxide phase is much less than that of AlN single crystal [3, 4], the thermal conductivity of sintered AlN is increased with a decreasing amount of grain boundary phases by sintering under a reducing atmosphere at higher sintering temperatures, and for longer sintering periods [5, 6]. On the other hand, Watari *et al.* [10] produced AlN specimens with various grain sizes, maintaining the oxygen content at a reasonably high level by ultra-high temperature hot isostatically pressed (HIPped) sintering, to study the relationships between the microstructure (i.e. grain size, amount and number of grain boundary phase) and thermal conductivity. They found that the room-temperature thermal conductivity of the HIPped AlN with a grain size of about 40 μm and an oxygen content of 0.9 wt % was 150 $W m^{-1} K^{-1}$, which was almost equal to that of pressureless-sintered AlN with a grain size of about 4 μm and oxygen content of 1.0 wt % [10]. Also the calculated room-temperature phonon mean free path of AlN ceramics and single crystal was about 10–40 nm, which is much smaller than the grain size [10, 11]. Therefore it can be concluded that the main controlling factor of thermal conduction for sintered AlN is not due to the grain boundaries and/or AlN

0022–2461

TABLE I Typical data on sintered AlN

Specimen	Sintering conditions	Thermal conductivity ($W\,m^{-1}\,K^{-1}$)	Oxygen content (wt %)	Grain size (μm)	Grain boundary phases
A	2173 K, 5 h	220	0.1	10	YN
B	2173 K, 1 h	175	0.6	6	YN
C	2073 K, 1 h	148	1.0	4	Y_2O_3, YN
D	1973 K, 1 h	121	1.4	3	$Al_2Y_4O_9$, Y_2O_3

grain size, but due to the internal structure of grains such as oxygen solute atoms and associated Al vacancies, for sintered AlN with a fairly good thermal conductivity and a low amount of grain boundary.

An insulating crystalline solid with a simpler structure, fewer lattice defects or a higher Debye temperature will show a higher thermal conductivity and longer phonon mean free path. At low temperatures a sintered body with defects will have a limited phonon mean free path at a magnitude which can correspond to the inter-defect distance. It is important to evaluate the phonon mean free path of sintered AlN at low temperatures in order to investigate the phonon scattering mechanism in the sintered body.

In this research, the thermal diffusivity of sintered AlN with various oxygen contents was measured at different temperatures ranging from 100 to 1000 K. From the results of thermal diffusivity the phonon mean free path was calculated in order to investigate the phonon scattering mechanisms.

2. Experimental procedure

A commercial AlN powder (F series, Tokuyama Soda, Tokyo) with an average particle size of 0.6 μm and a specific surface area of $3.2\,m^2\,g^{-1}$ was used in this research. According to the manufacturer, this powder contained 1 wt % oxygen, 220 p.p.m. carbon and trace amounts of iron, calcium and silicon. Y_2O_3 powder (ShinEtsu Chemicals, Tokyo) of 1 mol % (5.2 wt %) as sintering aid was added to the raw AlN powder.

These powders were mixed in a ball mill. After drying, the mixed powder was formed into pellets of 14 mm diameter and 8 mm height using a stainless steel die, and then cold isostatically pressed (CIPped) under 400 MPa for 60 s. The CIPped bodies were wrapped in carbon foil, and then sintered in a tungsten resistance furnace at temperatures of 1973, 2073 and 2173 K for 1 h under 0.1 MPa nitrogen gas atmosphere. The CIPped samples were also sintered at 2173 K for 5 h under the same atmosphere. The heating rate was $0.25\,K\,s^{-1}$ ($15\,K\,min^{-1}$) in all cases.

The bulk density was measured by a displacement method in water. The crystalline phase was identified by X-ray diffraction with CuK_α radiation. The oxygen content was measured by radioactive isotope analysis. The microstructure was examined by scanning electron microscopy (SEM). The AlN grain size was estimated from SEM photographs of fractured surfaces.

Discs of 10 mm diameter and 3.5 mm thickness were prepared to measure the thermal diffusivity at temperatures ranging from 100 to 1000 K under a vacuum of about 10^{-2} Pa or less by a laser flash method (TC-3000H, Shinku Riko, Yokohama). The equipment and detailed procedures for thermal diffusivity measurement by the laser flash technique have been described elsewhere [18].

The experimental thermal conductivity κ_m was calculated from the experimental thermal diffusivity α, heat capacity C_p and density D as

$$\kappa_m = \alpha C_p D \quad (1)$$

In this research, the reported values for AlN specific heat [19] was used to determine the thermal conductivity. The obtained thermal conductivity was corrected for the total porosity of the sintered AlN [20].

3. Results

The room-temperature thermal conductivity, oxygen content, grain size and grain-boundary phase of AlN specimens obtained are shown in Table I. As shown in Table I, the room-temperature thermal conductivity and grain size increased, and the oxygen content of sintered AlN decreased, with increasing sintering temperature and period. Furthermore the thermal conductivity increased from 121 to $220\,W\,m^{-1}\,K^{-1}$ as the oxygen content decreased from 1.4 to 0.1 wt %.

The X-ray diffraction analysis revealed that $Al_2Y_4O_9$ ($2Y_2O_3 \cdot Al_2O_3$) grain boundary phase of the sintered AlN transformed to Y_2O_3 and YN phases with increasing sintering temperature. A difference of grain boundary phases was observed between the surface and the interior of the AlN specimens. Grey YN powder was formed on the surface of the AlN ceramics sintered at 2073 and 2173 K after leaving in air for about 2 days at room temperature. These experimental results were previously reported by Watari *et al.* [8], and from these results the chemical reactions which lead to increased AlN thermal conductivity on decreasing oxygen content during sintering under a reducing nitrogen atmosphere with carbon were identified.

The temperature dependence of thermal diffusivity of the AlN specimens is shown in Fig. 1. The temperature dependence of thermal diffusivity is affected by the oxygen content; the specimens with a higher thermal diffusivity at low temperatures were those with a lower oxygen content.

Fig. 2 shows the temperature dependence of AlN thermal conductivity. The thermal conductivity increases rapidly at low temperature as the temperature augments, reaches a maximum at around 300 K, and

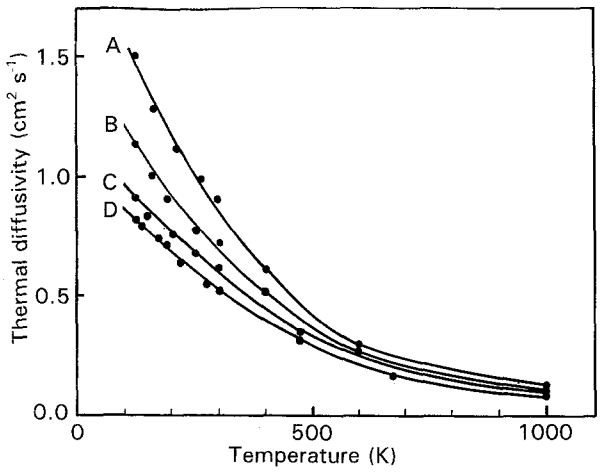

Figure 1 Thermal diffusivity versus temperature. Specimens A, B, C and D are as indicated in Table I.

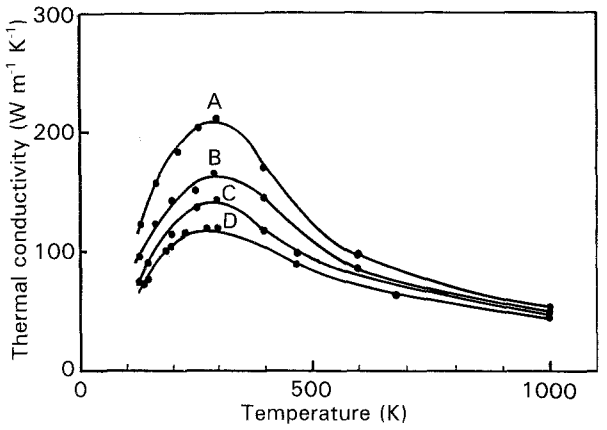

Figure 2 Thermal conductivity versus temperature. Specimens A, B, C and D are as indicated in Table I.

decreases thereafter with increasing temperature. The AlN specimen with a lower oxygen content has a higher thermal conductivity at any temperature.

4. Discussion

Phonons play a vital role in the thermal conduction of electrically insulating ceramic materials such as AlN, diamond, SiC and Si_3N_4. At high temperatures, the phonon mean free path decreases and the frequency of phonon scattering increases with increasing temperature because of phonon–phonon scattering. But at lower temperatures the phonon–phonon scattering in electrically insulating ceramic materials decreases, and then its thermal conduction mechanism is controlled by phonon–defect scattering and/or phonon–grain boundary scattering. At sufficiently low temperatures the phonon mean free path will be nearly equal to the inter-defect distance, grain size or specimen size. It is possible to estimate the mean inter-defect distance in the lattice of sintered AlN with crystalline defects from the calculated phonon mean free path at low temperatures. In this work, the phonon mean free path of sintered AlN was calculated from the present experimental results of thermal diffusivity. Furthermore the phonon–defect scattering distance was calculated from the phonon mean free path of sintered AlN in order to understand the mechanism of phonon scattering by oxygen-related defects in AlN grains of a sintered body. The resultant phonon mean free path l is given by

$$l = 3\kappa/VC \quad (2)$$

where κ is the resulting thermal conductivity, V the group velocity and C the specific heat capacity per unit volume [21]. Usually the group velocity is estimated to be the longitudinal sound velocity for this thermal conduction case. The phonon mean free path of sintered AlN can be calculated from Equation 2 with the thermal conductivity, the longitudinal sound velocity and the specific heat of sintered AlN. For the longitudinal sound velocity a value of 10^4 m s^{-1} was used for all temperatures [11]. The temperature dependence of the phonon mean free path of specimens A and D is shown in Fig. 3. The phonon mean free path is influenced by the temperature and oxygen content; specimens with lower oxygen content had a longer phonon mean free path at lower temperatures.

Slack *et al.* [2] measured the thermal conductivity of a high-purity single-crystal AlN with about 300 p.p.m. oxygen by weight at temperatures ranging from 0.4 to 1800 K, and they predicted the thermal conductivity of a pure AlN single crystal at those temperatures by correcting the residual oxygen content in a high-purity AlN single crystal. It is therefore considered that the thermal conductivity of a pure AlN single crystal is determined by the mean phonon–phonon scattering distance; also the phonon mean free path of a pure AlN single crystal is equal to the mean phonon–phonon scattering distance. In this work, the mean phonon–phonon scattering distance was calculated from Equation 2 with the thermal

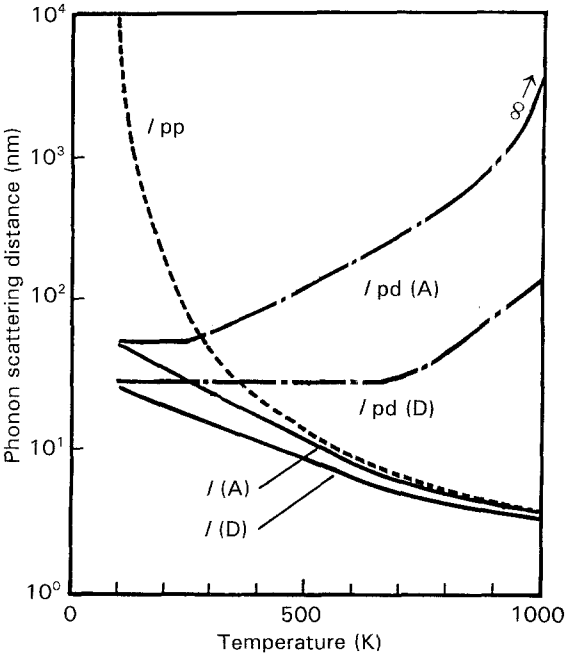

Figure 3 Temperature dependence of AlN phonon mean free path. $l_{(A)}$ and $l_{(D)}$ show the resultant phonon mean free path of specimens A and D. $l_{pd\ (A)}$ and $l_{pd\ (D)}$ show the mean phonon–defect scattering distance for specimens A and D. l_{pp} indicates the mean phonon–phonon scattering distance, calculated from AlN pure single-crystal data [2].

conductivity of pure AlN single crystal, and is shown in Fig. 3. The mean phonon–phonon scattering distance is about 3 μm at 100 K, 150 nm at 200 K, 40 nm at room temperature, 9 nm at 600 K and 4 nm at 1000 K. At low temperatures, the mean phonon–phonon scattering distance is longer than the phonon mean free path of sintered AlN with oxygen contents of 0.1 and 1.4 wt %, but at high temperatures the phonon mean free path of sintered AlN is close to the mean phonon–phonon scattering distance as shown in Fig. 3. These results show that at low temperatures the thermal conduction of sintered AlN is mainly due to the phonon–defect scattering and/or phonon–grain boundary scattering, and at high temperatures it is mainly due to the phonon–phonon scattering.

In heat transport, there are several phonon scattering processes such as phonon–phonon scattering, phonon–defect scattering, phonon–grain boundary scattering, phonon–boundary scattering, phonon–electron scattering and so on. It is proper to take the sum of the scattering probabilities for each mode. The frequency of phonon scattering V/l is expressed as

$$\frac{V}{l} = \sum_{i=l}\left(\frac{V}{l_i}\right) \tag{3}$$

or

$$\frac{V}{l} = \frac{V}{l_{pp}} + \frac{V}{l_{pd}} + \frac{V}{l_{pg}} + \frac{V}{l_{pb}} + \frac{V}{l_{pe}} \quad \ldots \tag{4}$$

where l_{pp} is the mean phonon–phonon scattering distance, l_{pd} the mean phonon–defect scattering distance, l_{pg} the mean phonon–grain boundary scattering distance, l_{pb} the mean phonon–boundary scattering distance and l_{pe} the mean phonon–electron scattering distance. Also the reciprocal phonon mean free path $1/l$ is the reciprocal sum of those from different scattering processes [21]:

$$\frac{1}{l} = \sum_{i=l}\left(\frac{1}{l_i}\right) \tag{5}$$

or

$$\frac{1}{l} = \frac{1}{l_{pp}} + \frac{1}{l_{pd}} + \frac{1}{l_{pg}} + \frac{1}{l_{pb}} + \frac{1}{l_{pe}} \quad \ldots \tag{6}$$

In the case of ceramic materials, the thickness of grain boundaries may determine whether the predominant phonon scattering site is at grain boundaries or occurs internally within AlN grains. If the grain boundary has a significant thickness, phonons will be scattered a few times inside the grain boundary phase and the thermal conductivity of the grain-boundary phase may play a significant role in the final thermal conductivity. If the grain boundaries are thin enough, a phonon may scatter once at the grain boundary and then phonon scattering sites in AlN grains will be the factor controlling the thermal conductivity of sintered AlN.

The difference between the thickness of the grain boundaries for these two cases is that in the former case the thickness of the grain boundary is at least a few times larger than the phonon mean free path. However, the grain boundary thickness of AlN ceramics with a thermal conductivity up to 100 W m^{-1} K^{-1} is about 2 nm [5, 16]. This thickness is much smaller than the phonon mean free path of sintered AlN at temperatures ranging from 100 to 1000 K, as shown in Fig. 3. Also high-resolution TEM shows a high content of AlN–AlN grain boundaries which show no second-phase material [17]. Therefore phonon scattering by the grain boundary phase is not the dominant mechanism controlling the thermal conductivity of conventionally prepared AlN ceramics. Furthermore, considering that oxygen-related internal defects in AlN grains are the controlling factor in the thermal conduction mechanism of a sintered body [10, 11], the frequency of phonon–grain boundary scattering is much smaller than that of phonon–defect scattering. Also in AlN ceramics there are no free electrons, so that the phonon–electron mechanism of thermal conduction can be neglected. Consequently the thermal conduction mechanism of sintered AlN is controlled by phonon–phonon scattering and phonon–defect scattering, and then the frequency of phonon scattering and the reciprocal phonon mean free path are given by

$$\frac{V}{l} = \frac{V}{l_{pp}} + \frac{V}{l_{pd}} \tag{7}$$

$$\frac{1}{l} = \frac{1}{l_{pp}} + \frac{1}{l_{pd}} \tag{8}$$

By using Equation 8 with the phonon mean free path of sintered AlN and the mean phonon–phonon scattering distance, the mean phonon–defect scattering distance for specimens A and D is calculated as shown in Fig. 3. The mean phonon–defect scattering distance decreases with decreasing temperature, and was limited to about 50 nm at temperatures ranging from 100 to 270 K for specimen A and about 30 nm at temperatures ranging from 100 to 700 K for specimen D. These limited phonon–defect scattering distances are much smaller compared to the AlN grain size of 1 to 10 μm as shown in Table I, and are much larger compared with the order of the dimensions of the AlN *a*-axis and *c*-axis lattice parameters (0.311 and 0.498 nm, respectively).

It is possible that the phonon–defect scattering distance relates closely to the distribution condition of oxygen-related defects in AlN grains. Recently Harris *et al.* [12, 13] proposed an oxygen-related defect evolution mechanism as a function of oxygen content from the results of photoluminescence spectroscopy, thermal conductivity measurements, X-ray diffraction lattice parameter measurements and transmission electron microscopy. They concluded that at low oxygen concentrations (region I), isolated oxygen impurities exist uniformly in the AlN lattice, then oxygen impurity and aluminium vacancy form a correlated defect, attracted together via a Coulombic interaction. At higher concentrations (region II) a slight change in the aluminium atom position annihilates the vacancy site and results in an octahedrally coordinated aluminium site, and at still higher oxygen levels (region III),

these octahedra organize to form extended defects such as inversion domain boundaries (IDBs) and oxygen-containing stacking faults [12, 13].

Actually, in region III, curved IDBs and a number of planar stacking faults within an AlN grain of a sintered body were observed by Harris *et al.* [12, 13]. But the magnitude of the dimension of IDBs is of the order of micrometres, which is too big to compare with the limited phonon–defect scattering distance. In region II, the thermal conduction mechanism is determined by the phonon scattering due to an Al–O octahedral defect-cluster unit. If the Al–O unit is approximated as a fragment of Al_2O_3 with dimensions of the order of the Al_2O_3 a axis, its value is about 0.513 nm, which is much smaller than the mean phonon–defect distance. Therefore it is considered that the AlN grains of the sintered body obtained in this work as well as all commercially available AlN ceramics have a low oxygen concentration (region I), and the isolated oxygen-related defects (i.e. Al vacancies) are separated uniformly from each other by a distance of about 50 nm in the AlN lattice.

From the mean phonon–phonon scattering distance and phonon–defect scattering distance, the frequency of phonon scattering is calculated by using Equation 7, and is shown in Fig. 4. The value of V/l_{pp} determined by phonon–phonon scattering decreases with decreasing temperature. However, the value of V/l_{pd} determined by phonon–defect scattering is limited to a value of 2×10^{11} s^{-1} at temperatures below 270 K for specimen A, and a value of 3.5×10^{11} s^{-1} at temperatures below 700 K for specimen D.

Fig. 5 shows the ratio of phonon–phonon and phonon–defect scattering frequencies in specimens A and D against temperature. The phonon scattering is

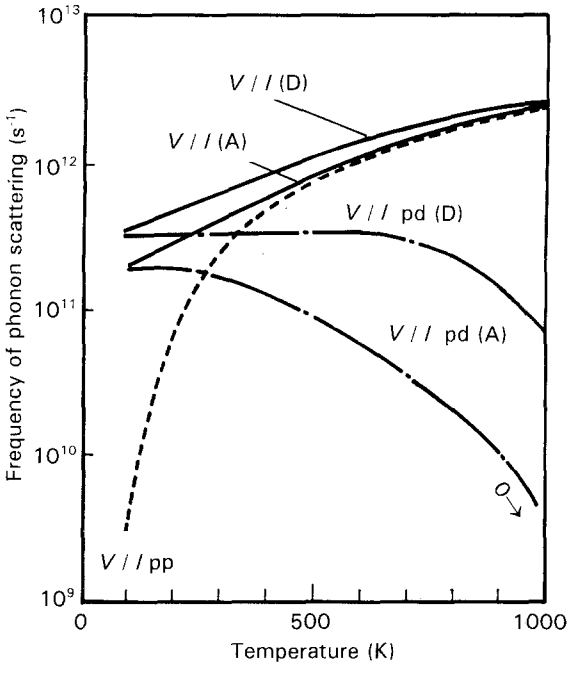

Figure 4 The mean frequency of phonon scattering in AlN ceramics. $V/l_{(A)}$ and $V/l_{(D)}$ are the total mean frequency of phonon scattering for specimens A and D. $V/l_{pd\ (A)}$ and $V/l_{pd\ (D)}$ show the mean frequency of phonon–defect scattering for specimens A and D. V/l_{pp} indicates the mean frequency of phonon–phonon scattering.

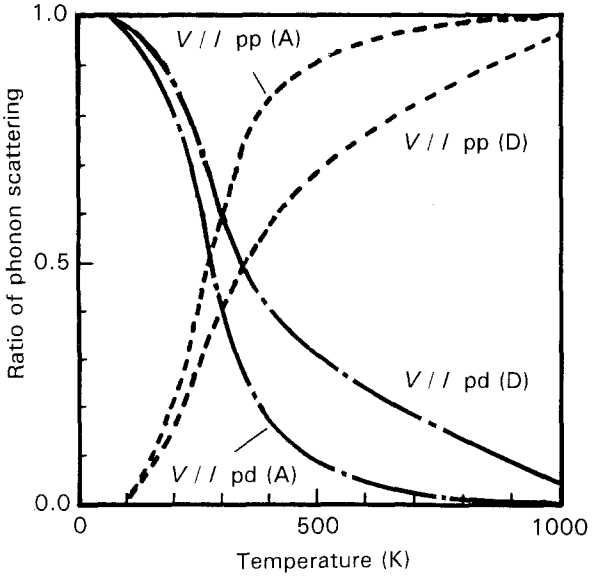

Figure 5 Ratios of phonon–phonon and phonon–defect scattering frequencies in sintered AlN.

mainly due to the phonon–defect scattering process at temperatures below 270 K for specimen A and at temperatures below 350 K for specimen D. Therefore the thermal conductivity of the AlN specimen with a higher oxygen content is controlled by phonon–defect scattering at higher temperatures.

5. Conclusions

The thermal diffusivity of AlN ceramics with various oxygen contents was measured at different temperatures ranging from 100 to 1000 K. From the results for the thermal conductivity of sintered and pure single-crystal AlN, calculations were made of the phonon mean free path, the mean phonon–phonon scattering distance and the mean phonon–defect distance, in order to investigate the phonon scattering mechanisms. From the present work, the following conclusions were drawn:

1. The calculated separation of oxygen-related defects in AlN grains is about 50 nm for a specimen with an oxygen content of 0.1 wt% and a room-temperature thermal conductivity of 220 W m^{-1} K^{-1}, and is about 30 nm for a specimen with an oxygen content of 1.4 wt % and a room-temperature thermal conductivity of 121 W m^{-1} K^{-1}. From the value of the separation of oxygen-related defects, it is considered that isolated aluminium vacancies with associated oxygen atoms are distributed uniformly in the AlN lattice.
2. The phonon scattering is mainly due to the phonon–defect scattering process at temperatures below 270 K for an AlN specimen with an oxygen content of 0.1 wt %, and at temperatures below 350 K for a specimen with an oxygen content of 1.4 wt %.
3. The temperature dependence of thermal diffusivity and conductivity is affected by the oxygen content; the specimen with higher thermal diffusivity and conductivity at low temperatures was that with the lower oxygen content.

References

1. G. A. SLACK, *J. Phys. Chem. Solids* **34** (1973) 321.
2. G. A. SLACK, R. A. TANZILLI, R. O. POHL and J. W. VANDERSANDE, *ibid.* **48** (1987) 641.
3. T. SAKAI, M. KURIYAMA, T. INUKAI and T. KIJIMA, *J. Ceram. Soc. Jpn* **86** (1978) 174.
4. N. KURAMOTO, H. TANIGUCHI, Y. NUMATA and I. ASO, *ibid.* **93** (1985) 517.
5. Y. KUROKAWA, K. UTSUMI and H. TAKAMIZAWA, *J. Amer. Ceram. Soc.* **71** (1988) 588.
6. M. OKAMOTO, H. ARAKAWA, M. OOHASHI and S. OGIHARA, *J. Ceram. Soc. Jpn* **97** (1989) 1478.
7. A. V. VIRKAR, T. B. JACKSON and R. A. CUTLER, *J. Amer. Ceram. Soc.* **72** (1989) 2031.
8. K. WATARI, M. KAWAMOTO and K. ISHIZAKI, *J. Mater. Sci.* **26** (1991) 4727.
9. K. ISHIZAKI and K. WATARI, *J. Phys. Chem. Solids* **50** (1989) 1009.
10. K. WATARI, K. ISHIZAKI and T. FUJIKAWA, *J. Mater. Sci.* **27** (1992) 2627.
11. K. ISHIZAKI, K. WATARI and T. FUJIKAWA, *Trans. Mater. Res. Soc. Jpn.*, **3** (1992) 1.
12. J. H. HARRIS, R. A. YOUNGMAN and R. G. TELLER, *J. Mater. Res.* **5** (1990) 1763.
13. R. A. YOUNGMAN and J. H. HARRIS, *J. Amer. Ceram. Soc.* **73** (1990) 3238.
14. T. YAGI, K. SHINOZAKI, N. MIZUTANI, M. KATO and A. TSUGE, *J. Mater. Sci.* **24** (1989) 1332.
15. S. HAGEGE, Y. ISHIDA and S. TANAKA, *J. Ceram. Soc. Jpn* **96** (1988) 1119.
16. D. L. CHALLAHAN and G. THOMAS, *J. Amer. Ceram. Soc.* **73** (1990) 216.
17. T. B. JACKSON, A. V. VIRKAR, K. L. MORE and R. A. CUTLER, presented at 92nd Annual Meeting of the American Ceramic Society, Dallas, Texas, April 1990, "Substrates for Electronics" paper no. 11-E-90.
18. K. WATARI, Y. SEKI and K. ISHIZAKI, *J. Ceram. Soc. Jpn* **97** (1989) 174/*J. Ceram. Soc. Jpn. Int. Edn* **97** (1989) 170.
19. D. R. STULL and H. PROPHET (eds), JANAF Thermochemical Tables, 2nd edn, National Standard Reference Data System (National Bureau of Standards, Washington, DC, 1971) p. 90.
20. W. D. KINGERY, H. K. BOWEN and D. R. UHLMANN, "Introduction to Ceramics" (Wiley, New York, 1960 p. 504).
21. J. M. ZIMAN, "Electrons and Phonons" (Oxford University Press, London, 1960) Ch. VIII.

Received 6 August 1991
and accepted 7 May 1992